



NOVA

University of Newcastle Research Online

nova.newcastle.edu.au

Zhou, Cheng; Tremain, Priscilla; Doroodchi, Elham; Moghtaderi, Behdad; Shah, Kalpit.
'A novel slag carbon arrestor process for energy recovery in steelmaking industry'.
Published in *Fuel Processing Technology* Vol. 155, p. 124-133 (2017)

Available from: <http://dx.doi.org/10.1016/j.fuproc.2016.05.006>

© 2017. This manuscript version is made available under the CC-BY-NC-ND 4.0 license
<http://creativecommons.org/licenses/by-nc-nd/4.0/>

Accessed from: <http://hdl.handle.net/1959.13/1346650>

1 A Novel Slag Carbon Arrestor Process for Energy
2 Recovery in Steelmaking Industry

3 *Cheng Zhou, Priscilla Tremain, Elham Doroodchi, Behdad Moghtaderi*, Kalpit Shah**

4 Priority Research Centre for Frontier Energy Technologies & Utilisation

5 Discipline of Chemical Engineering, School of Engineering,

6 Faculty of Engineering and Built Environment,

7 The University of Newcastle, Callaghan, NSW 2308, Australia

8
9 ABSTRACT

10 A novel slag carbon arrestor process (SCAP) was proposed to improve the heat recovery in energy-
11 intensive steelmaking process, which typically has a low heat recovery. The proposed SCAP process
12 introduces a tar reformer to utilise the slag - a by-product from steelmaking process - as the catalyst to
13 convert coke oven gas and tar into hydrogen-enriched fuel gas. This is achieved by making use of the
14 valuable carbon and/or energy contained in the coke oven gas, which otherwise being wasted, to assist

* Corresponding authors; Dr. Kalpit Shah. Email: Kalpit.Shah@newcastle.edu.au.

Behdad Moghtaderi. Ph: +61-2-4985-4411; Fax: +61-2-4921-6893. E-mail address: Behdad.Moghtaderi@newcastle.edu.au

15 in tar reforming and produce hydrogen-enriched gas. Such concept is expected to reduce the undesired
16 tar formation in steelmaking process along with improved heat recovery efficiency and higher quality
17 coke oven gas production. Both simulation and experimental studies on the slag carbon arrestor process
18 were performed. The preliminary thermodynamic analysis carried out using Aspen Plus v8.4 indicates
19 that with the tar reformer the energy content of coke oven gas was found increased from ~34.6 MJ/kg
20 to ~37.7 MJ/kg (or by 9%). Also, with the utilisation of carbon deposition on the slag, a reduction of up
21 to 12.8% coke usage in the steelmaking process can be achieved. This corresponds to an energy saving
22 of 4 % and a carbon emission reduction of 5.7 % compared with the conventional steelmaking process.
23 Preliminary experimental TGA-FTIR investigations revealed a reduction in the aromatic and aliphatic
24 hydrocarbon groups and an increase in the production of CO₂ and CO, attributed to the tar cracking
25 abilities of slag.

26

27 KEYWORDS: slag carbon arrestor process (SCAP), steelmaking, carbon deposition, tar, coke oven gas.

28

29 **1 INTRODUCTION**

30 Steel production is a major indicator for economy growth especially for developing countries.

31 However, steel making is a highly energy intensive process accounting for nearly 5% of the world's

32 total energy consumption and approximately 6.7% of total world CO₂ emissions. Also, the heat

33 recovery in a steel making process is typically low at only ~17% [1]. The rising cost of energy and

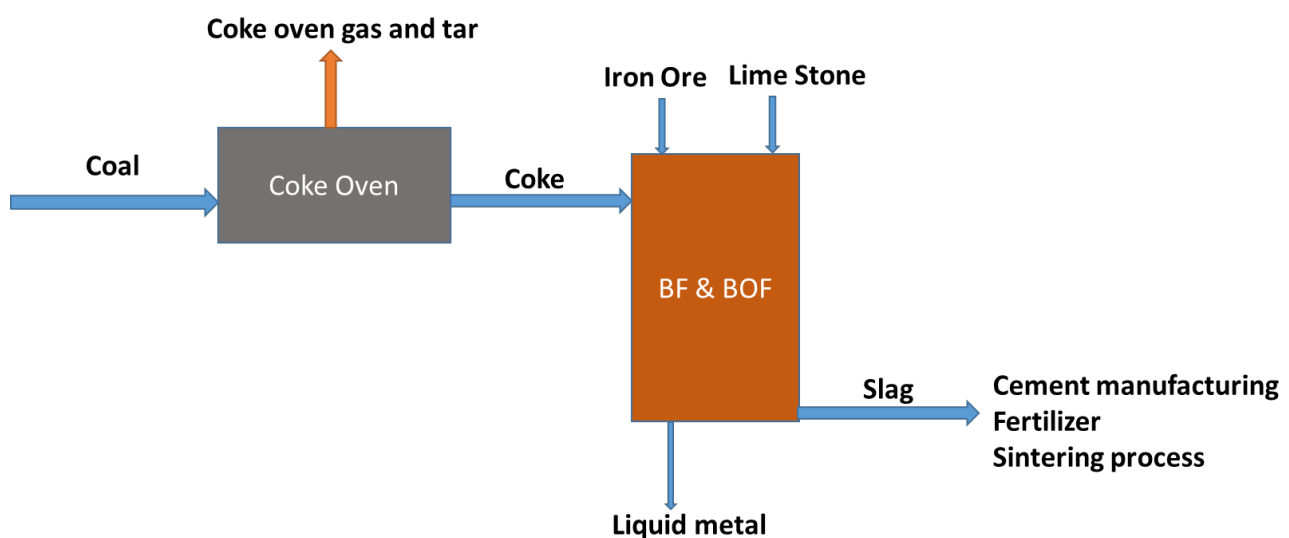
34 high demand for greenhouse gas emission reductions represent major challenges for the steel
35 industry.

36 Currently, approximately 17% of the operating cost of the steelmaking industry is energy. This energy
37 originates from multiple sources, such as coal, electricity, natural gas, recycled coke oven gas (COG)
38 and blast furnace gas (BFG) [2]. Recycling of waste heat and recovery of energy rich by-products
39 from these energy sources are identified as key measures to improve energy efficiency and reduce
40 costs and emissions of the modern-day steelmaking process. It is estimated that the energy recycled
41 from COG supplies ~20% of the total energy consumed in the present steelmaking process, with
42 potential of increasing to 40% if fully utilised. BFG, on the other hand, has the potential to supply up
43 to another 40% of the total plant energy consumption despite its low energy density (~ 1/3 of that of
44 COG) [3].

45 Motivated by this path, our research team at the University of Newcastle, Australia developed a novel
46 Slag Carbon Arrestor Process (SCAP) to improve the energy recovery of the steelmaking industry.
47 The work is also part of a major research theme on low-emission energy technology options [4-10]
48 being developed at the University of Newcastle, Australia. The SCAP process is to be introduced in the
49 following texts.

50 Figure 1 shows the conventional steel production process which primarily consists of two integrated
51 unit operations: coke production and iron ore reduction. The coke making process involves
52 carbonization of coal at high temperatures (800 - 1200°C) in an oxygen deficient atmosphere in order

53 to concentrate the carbon. During the coke making process, hot COG along with unwanted aromatic
54 hydrocarbon compounds (i.e. tar) are generated, which contain valuable carbon and energy [1]. The
55 produced COG is considered to be a good fuel source [11]. However, to ensure effective utilisation of
56 COG, tar must be removed as it can create operational problems such as condensation and pipe
57 blockages [11, 12]. To achieve this, the hot COG, at temperatures between 800 and 850°C, emitted
58 from coke ovens is spray cooled with an aqueous ammonia solution in order to remove most of the
59 higher hydrocarbons in the tar, such as benzene (C₆H₆), toluene (C₇H₈), and naphthalene (C₁₀H₈) etc. In
60 addition, complex processing plants are required for the conversion of tar into valuable chemical by-
61 products [13]. These processes, as mentioned by Yue et al. [14], cause significant heat losses and
62 serious secondary pollution due to tar losses in the waste water. Therefore, instead of physically and
63 chemically separating tar from COG, it would be highly beneficial if the tar could be decomposed into
64 light fuel gases in-situ with the assistance of a catalyst. The heat and chemical energy embodied in the
65 hot COG can also be used in this process.



66

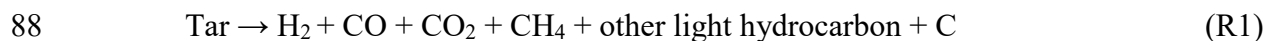
67 Figure 1: Process flow diagram of a conventional steelmaking process (BF & BOF: blast furnace &
68 basic oxygen furnace).

69 After the coke making process, iron ore reduction and steel production occur in the blast furnace (BF)
70 and basic oxygen furnace (BOF), respectively. Coke, sinter, and limestone are added in these two
71 furnaces. The purpose of the blast furnace is to chemically reduce iron oxides into liquid metal and
72 physically separate the liquid metal from slag. The operation of the blast furnace and basic oxygen
73 plant usually results in the production of a high amount of slag, containing high amounts of CaO, FeO,
74 SiO₂ and Al₂O₃ [15]. The majority of slag produced is currently used in the cement industry or as a
75 fertilizer, while a fraction of the slag is recycled in the sintering process and in the blast furnace for
76 supplying limestone and iron [16]. Heat recovery from slag is generally low and difficult due to its low
77 thermal conductivity between 0.1 - 3 W/mK [17]. In general, this contributes to the low heat recovery
78 of the steelmaking industry.

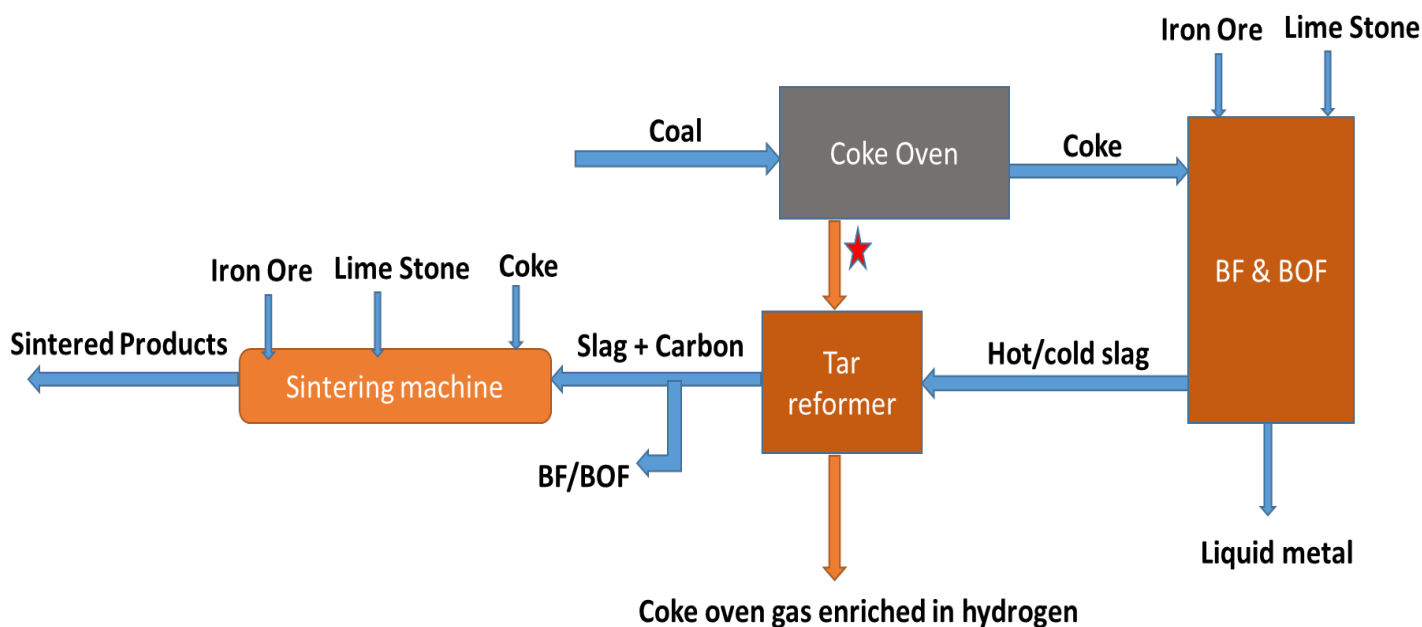
79 To overcome the aforementioned issues such as low heat recovery, high heat losses, and possible
80 secondary pollution, several options have been suggested in the literature such as hot-slag heat
81 recovery and more efficient process design [18]. Nonetheless those options are not fully developed for
82 commercial implementation. As a step change solution, a novel Slag Carbon Arrestor Process (SCAP)
83 was developed.

84 Figure 2 shows the proposed SCAP process in which a tar reformer is introduced to the conventional
85 steelmaking process. It is essentially the integration of a conventional steelmaking process and a tar

86 reforming/hydrogenation process. In the tar reformer, tar decomposes under a catalytic reaction with
 87 steelmaking slag (see reaction R1) while COG is converted into a hydrogen-enriched gas [19],



89 Normally very high temperatures are required for tar decomposition; catalysts such as steelmaking slag
 90 can help to reduce such temperatures. Generally, calcium and iron are considered to be favourable
 91 catalyst materials for pyrolysis, reforming or decomposition of coal and/or tar as well as hydrogen-
 92 enriched gas production [20]. The innovativeness of the SCAP process is that the tar reforming process
 93 makes use of slag, which is rich in calcium and iron oxides, in the place of traditional calcium/iron
 94 oxide catalysts.



95
 96
 97 Figure 2: Process flow diagram of the Slag Carbon Arrestor process for steelmaking (BF & BOF: blast
 98 furnace & basic oxygen furnace; the star sign: potential energy recovery point).

99 The slag entering into the tar reformer is best in the form of granulated slag (providing more surface
100 area for catalytic reaction), which is a sand-like product produced using instant quenching of molten
101 slag. Nevertheless, hot molten slag / rock type slag (produced by slowly cooling the molten slag)
102 should not be excluded for future study. Also generated along with the tar reforming process is a
103 possible soot formation/carbon deposition on the surface of slag, which can then be recycled back to
104 the sinter machine and blast furnace. With such carbon recycling, the SCAP process is expected to not
105 only reduce coke consumption in the steelmaking process, but also eliminate tar associated problems as
106 well as the production of a hydrogen-enriched COG. Another advantage of SCAP process is that it can
107 be readily retrofitted to existing steel production plants.

108 The objective of this paper was to study the feasibility of the SCAP process by (i) investigating via
109 simulations the extents of COG quality improvement, carbon deposition and tar decomposition (ii)
110 conducting energy and mass balance analyses of the process, (iii) examining the effect of tar
111 decomposition extent on carbon deposition, energy saving, and emission reduction potentials, and (iv)
112 using preliminary experiments to confirm the concept and verify simulation results.

113

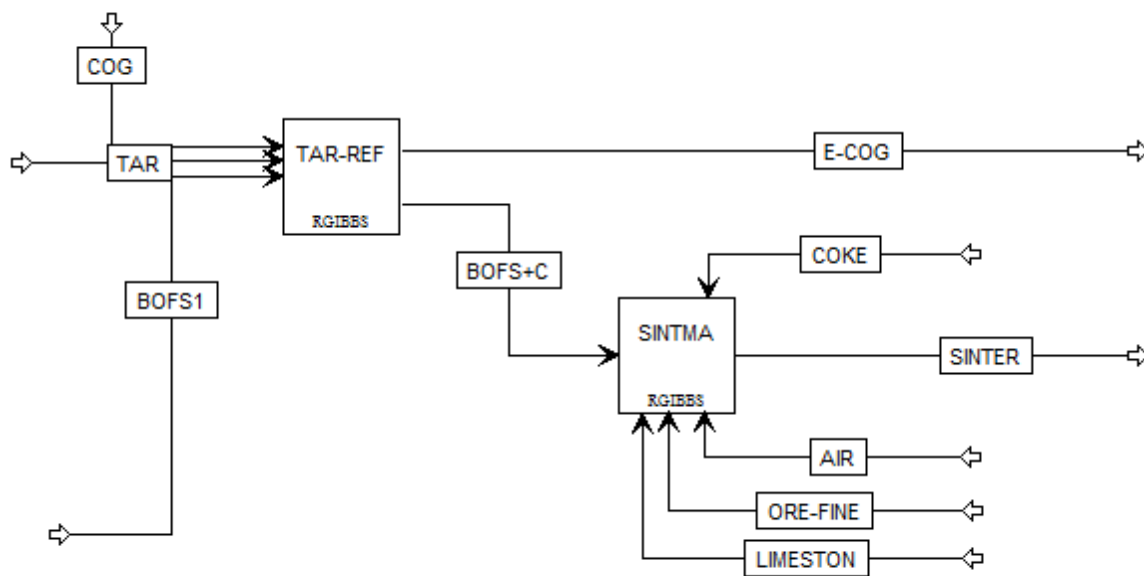
114 **2 METHODOLOGY**

115 **2.1 Process Simulation**

116 The process simulation was carried out using the process simulation package - Aspen Plus v8.4. The
117 Aspen model solves all the equilibrium constant equations simultaneously and calculates the
118 equilibrium conditions by minimizing the total Gibbs free energy of the system. Moreover,
119 thermodynamic database - HSC chemistry (developed by Outotec) - was also used as an assisting tool.
120 With the above tools, energy and mass balance analyses were performed for the SCAP process.

121 Figure 3 shows the process flow diagram of the SCAP model. The SCAP model was developed and
122 designed at a steel production rate of one tonne/hr and based on the typical conditions of the
123 conventional steelmaking process. Specifically, in the simulation it was assumed that for the production
124 of one tonne of steel it requires 243 kg of coke and 140 kg of sinter in the blast furnace for iron
125 production [21]. To produce the 140 kg of sinter, approximately 3.9 kg of recycled BOF slag and 5 kg
126 of coke breeze was consumed [22], whilst the production of 243 kg of coke generates approximately
127 66.6 kg of hot raw COG (excluding tar) and 13.3 kg of tar [23]. The production of one tonne of steel
128 also generates about 180 kg of BOF slag and 375 kg of blast furnace slag [24]. However, due to the
129 harmful constituents (Na_2O , K_2O and S) in the blast furnace slag, it is not recycled in the steelmaking
130 process while up to 25% of BOF slag can be recycled back to the sinter machine, basic oxygen plant
131 and blast furnace [25]. These data are based on and crosschecked with multiple literature [24, 26, 27].

132 The above data also indicates that the typical coke consumption of a sinter machine is only ~2% of the
 133 total coke usage for the steelmaking process, and thus coke saving in the sinter machine has a practical
 134 limit on the maximum saving that could be achieved. In contrast, the major energy saving that may be
 135 contributed by the SCAP process is more related to the recycled BOF slag in the basic oxygen plant
 136 and blast furnace. Here, the carbon-deposited BOF slag may help reduce coke usage in the blast
 137 furnace and the potential for this saving is far greater than the coke saving in the sinter machine. Based
 138 on the above discussion, the amount of BOF slag used in the simulation was fixed at 45 kg per tonne of
 139 steel production, including 41.1 kg of recycled BOF slag to the blast furnace [24, 25] and 3.9 kg to the
 140 sinter machine [22].



141
 142 Figure 3: Aspen Plus process flow diagram of the proposed SCAP concept (E-COG: hydrogen-
 143 enriched COG; TAR-REF: tar reformer; SINTMA: sinter machine).

144 The operating temperature of the tar reformer was fixed at 600°C with an inlet COG temperature at
 145 800°C. These temperatures were chosen based on the literature which suggests the optimum

146 temperatures of coal pyrolysis and tar decomposition for achieving the maximum carbon deposition
147 [28]. Table 1 gives the detailed compositions of the hot raw COG (excluding tar) and BOF slag used in
148 this study. It should be highlighted that the hot raw COG used in this study is the uncooled raw oven
149 gas emitted directly from the coke oven battery, rather than the conventional cooled COG obtained
150 from the gas collection main after tar removal. The hot raw COG composition in Table 1 however does
151 not include tar, the composition of which is to be identified separately. Before simulating the tar
152 component in the COG, it should be noted that coal tars are extremely complex mixtures consisting of
153 greater than 400 components. These components again vary considerably according to the nature of the
154 coal charge and the coal carbonisation conditions [29]. A simple yet effective way to simulate coal tar
155 in Aspen Plus was reported by Hamelinck et al. [30] based on the C:H atomic ratio of most coal tar
156 (1.4:1) [11]. In his approach (also adopted in this study) the composition of tar was represented by
157 phenanthrene (C₁₄H₁₀) which has a similar C:H atomic ratio and thermo-physical properties with tar
158 [30]. The yield of tar per tonne of dry coal is about 30-50 litres (or 3.5 - 5.9 wt% of dry coal) [27],
159 whilst the yield of tar per one standard m³ of hot raw COG (without tar) is typically 100 g/m³ [26]. In
160 this study the tar content of the hot raw COG (excluding tar) was fixed at the typical value of 100 g/m³
161 or 20 wt%. A tar conversion rate of 0 - 100% in the tar reformer was examined. Further, a cold
162 granulated BOF slag with a temperature of 25°C was used. Utilising the heat from the hot slag directly
163 for tar reforming reactions is expected to further improve heat recovery. However, this aspect was not
164 examined in the present study.

165 Table 1: Composition of hot raw COG and BOF slag.

Hot raw COG* (excluding tar)	Fraction (vol%)	BOF slag**	Composition (wt%)
H ₂ O	10.41	Ca ₂ Fe ₂ O ₅	10
H ₂	49.28	Ca ₂ SiO ₄	45
CH ₄	26.75	FeO	25
CO	5.50	CaO	5
CO ₂	2.28	Ca ₃ SiO ₅	15
N ₂	2.19	-	-
C ₂ H ₄	1.61	-	-
C ₂ H ₆	0.82	-	-
C ₃ H ₆	0.05	-	-
H ₂ S	0.47	-	-
NH ₃	0.66	-	-
Total	100	Total	100

*. Based on reference [11]; **.Based on reference [31].

2.2 Experimental

A series of preliminary coal and coal-slag pyrolysis experiments were completed. The apparatus, presented in Figure 4, consisted of a thermo-gravimetric analyser coupled with a Fourier Transform Infrared Spectrometer (TGA-FTIR) to allow for online mass loss and gas evolution characterisation. An Australian bituminous coal was used in all experiments, with proximate and ultimate analyses of the coal presented in Table 2. A synthetic slag, with a composition of CaO: FeO: SiO₂:Al₂O₃ = 0.45:0.3:0.2:0.05 and particle size of 75-212 μm , was used in experiments and was calcined in nitrogen at 800°C for 1 hr prior to experiments.

175

Table 2: Proximate and ultimate analysis of coal used in this study

	Proximate Analysis ^a				Ultimate Analysis				
	M (%)	A (%)	VM (%)	FC (%)	C (%)	H (%)	N (%)	S (%)	O ^b (%)
coal	3.7	8.9	32.7	58.4	77.2	5.2	2.0	0.7	15

176

a - On a dry basis, with M, moisture; A, ash; VM, volatile matter; and FC, fixed carbon.

177

b - O calculated by difference.

178

TGA conditions for all experiments consisted of a nitrogen sweep gas flow rate of 100 mL/min, ramp

179

rate of 10°C/min and final pyrolysis temperature of 900°C. FTIR scans were taken at 10°C intervals

180

and operating conditions consisted of a gas cell length of 10 cm and temperature of 240°C, transfer line

181

temperature of 240°C, 32 scans per spectra for a scan range of 500 – 4000 cm⁻¹ and resolution of 4 cm⁻¹

182

¹. Experimental scenarios examined were coal pyrolysis without slag and coal pyrolysis with slag at

183

mass ratios of 6.75:1 (the same ratio used in the simulation), 1:1 and 1:3 of coal to slag respectively.

184

185

186

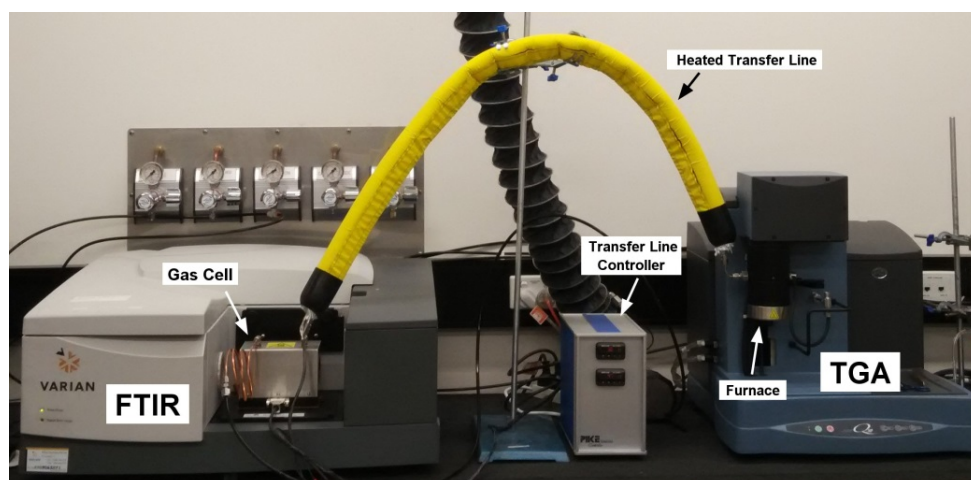


Figure 4: Experimental TGA-FTIR setup.

187 2.3 Performance Indicators

188 The advantages of the proposed SCAP process over the conventional steelmaking process were
189 investigated by evaluating some of the key performance indicators, including COG quality
190 improvement, carbon deposition and coke reduction rate, energy saving, and emission reduction.

191 2.3.1 COG quality improvement

192 Depending on the extent of COG reforming and the tar decomposition reaction, the energy content of
193 the reformed COG varies accordingly. To quantify such improvement, Equation (1) was used, namely,

$$194 \text{ COG quality improvement} = \frac{E_{COG}}{E_{COG,0}} - 1 \quad (1)$$

195 where $E_{COG,0}$ denotes the energy content of the hot raw COG (excluding tar) and E_{COG} denotes the
196 energy content of the reformed COG.

197 2.3.2 Carbon deposition and coke saving

198 The amount of deposited carbon on the slag was expressed in terms of a mass fraction of the reacted
199 slag/hot raw COG. The associated coke saving that may be achieved directly in the SCAP process was
200 calculated by,

$$201 \text{ Direct coke saving} = \frac{m_{coke,0} - m_{carbon} \times E_{carbon} / E_{coke}}{m_{coke,0}} \quad (2)$$

202 where $m_{coke,0}$ is the conventional coke consumption, m_{carbon} is the amount of deposited carbon, E_{carbon}
203 and E_{coke} are respectively the energy contents of pure carbon and coke, taken as 33 MJ/kg and 29 MJ/kg,
204 respectively.

205 In addition, there may also be some forms of indirect coke saving that may be achieved in the SCAP
206 process owing to the improved energy recovery, which is quantified by,

$$207 \text{ Indirect coke saving} = \frac{m_{coke,0} - Q_{saving}/E_{coke}}{m_{coke,0}} \quad (3)$$

208 where Q_{saving} is the thermal energy saving that may be achieved in the SCAP process yet is generally
209 unavailable for recovery in the conventional steelmaking process.

210 2.3.3 Energy saving and emission reduction

211 The total energy saving of the SCAP process per tonne of steel was calculated against the average
212 energy intensity of the conventional steelmaking process at 21 GJ/tonne of steel. The associated
213 emission reduction was estimated by converting both direct and indirect coke savings to an equivalent
214 CO₂ saving, which were then compared with the typical emission intensity of the conventional
215 steelmaking process at 1.8 tonne CO₂/tonne of steel.

216

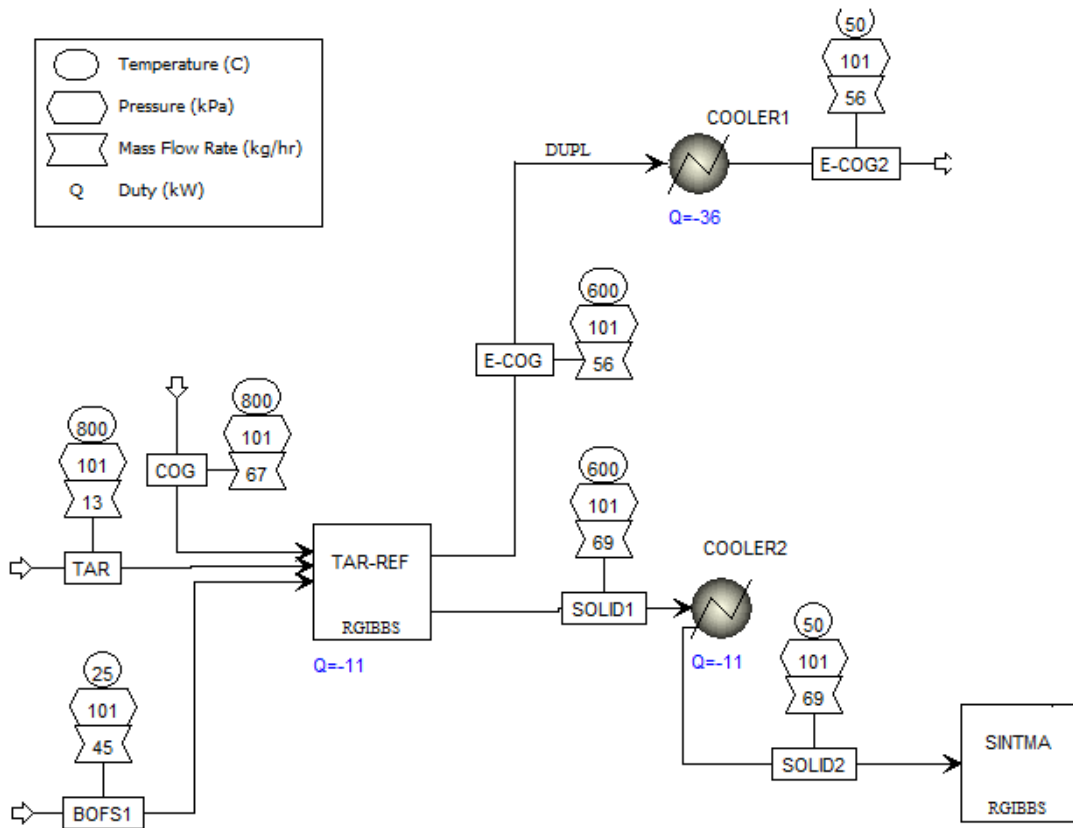
217 **3 RESULTS AND DISCUSSION**

218 The simulation and experimental results are presented in Sections 3.1 and 3.2, respectively.

219 **3.1 Simulation**

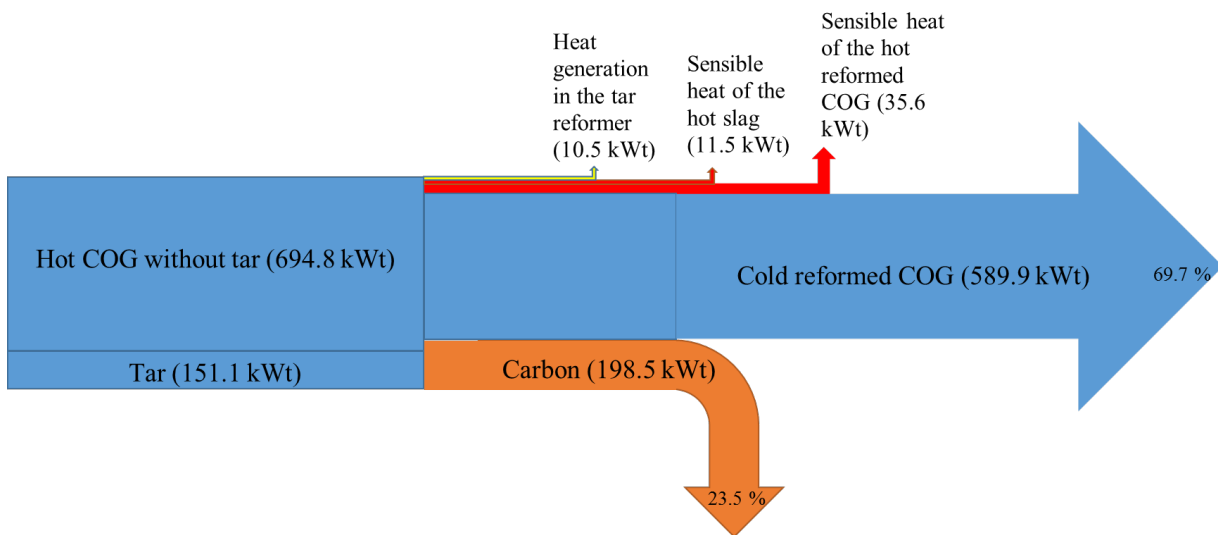
220 3.1.1 Energy and mass balance

221 Figure 5 shows the heat and mass balance analysis of the SCAP process, designed based on a capacity
222 of one tonne/hr of steel production. A quick mass balance analysis shows that at a tar reformer
223 temperature of 600°C and assuming a complete tar conversion, the weight of BOF slag was found to
224 increase from 45 kg/hr to 69 kg/hr while the amount of COG reduced from 67 kg/hr to 56 kg/hr. These
225 changes were confirmed to be owing to carbon deposition on the slag. The heat balance analysis shows
226 that a noticeable part of the sensible and chemical energy stored in the hot raw COG and tar was
227 transformed into the chemical energy in the deposited carbon, whilst the rest was kept with the
228 reformed COG, the sensible heat of the hot reacted slag, and in the form of reaction heat. A more
229 detailed analysis of the energy flows in the SCAP process is presented in Figure 6 via a Sankey chart.



230

231 Figure 5: Heat and mass balance of SCAP process at a tar reformer temperature of 600°C and assuming
 232 100% tar conversion (E-COG: hydrogen-enriched COG; TAR-REF: tar reformer; SINTMA: sinter
 233 machine).



234

235 Figure 6: Sankey diagram of the energy flows in SCAP process at a tar reformer temperature of 600°C.

236 Figure 6 shows that ~19% of the total energy input of the process comes from tar. Upon successful
 237 conversion and utilisation, such energy can be recovered and transformed into energy in the form of

238 carbon to be more effectively utilised. Some carbon also derives from the methane content of the COG,
239 which in total contributes to a net carbon energy output of ~23.5% of the total energy input (see Figure
240 6). This portion of energy can be directly used to offset coke usage in the sinter plant and blast furnace.
241 The reformed COG was found to contain ~69.7% of the total energy input, which is believed to be a
242 more valuable fuel than the conventional COG as it is now hydrogen-enriched. Also, the sensible heat
243 contained in the hot COG and slag, although insignificant and mostly wasted in the conventional
244 steelmaking process, may easily find a recovery path in the proposed SCAP process.

245 3.1.2 COG quality improvement

246 Table 3 gives the gas composition of COG before and after the tar reformer at a reforming temperature
247 of 600°C for both 0% and 100% tar conversion rates. The results show that with the newly installed tar
248 reformer, the SCAP process can greatly increase the hydrogen content of the COG from about 49% to
249 63% assuming that the tar remains intact (i.e. 0% tar conversion) while 64% assuming that the tar was
250 completely decomposed (100% tar conversion). This indicates that COG reforming was the main reason
251 for hydrogen enrichment instead of tar decomposition. The decreasing methane content from about 27%
252 to 18% was attributed to the reaction converting methane into the deposited carbon on the slag and H₂.
253 On the other hand, the decreasing CO₂/CO contents can be mainly attributed to the carbonation of free
254 CaO contained in the slag. C₂ and C₃ hydrocarbons were also found completely reacted in the tar
255 reformer. The above changes in the gas composition of COG are expected to result in an improved
256 energy quality of the COG, which was quantified in the following study.

257 Table 3: Gas composition of COG before and after tar reformer at a reforming temperature of 600°C.

Gas composition (vol%)	Raw COG (tar excluded)	Reformed COG	
		0% tar conversion	100% tar conversion
H ₂ O	10.41	10.25	10.05
H ₂	49.28	63.30	64.36
CH ₄	26.75	17.50	18.09
CO	5.50	3.67	3.54
CO ₂	2.28	1.60	1.49
N ₂	2.19	2.27	2.20
C ₂ H ₄	1.61	0.00	0.00
C ₂ H ₆	0.82	0.00	0.00
C ₃ H ₆	0.05	0.00	0.00
H ₂ S	0.47	0.25	0.25
NH ₃	0.66	0.01	0.01
Tar	0.0	1.14	0.0

258

259 Table 4: Gas composition of the reformed COG and deposited carbon on the slag as a function of the
 260 amount of slag participating in the reaction (100% slag = 45 kg/hr, tar reforming temperature: 600°C,
 261 tar conversion rate: 100%).

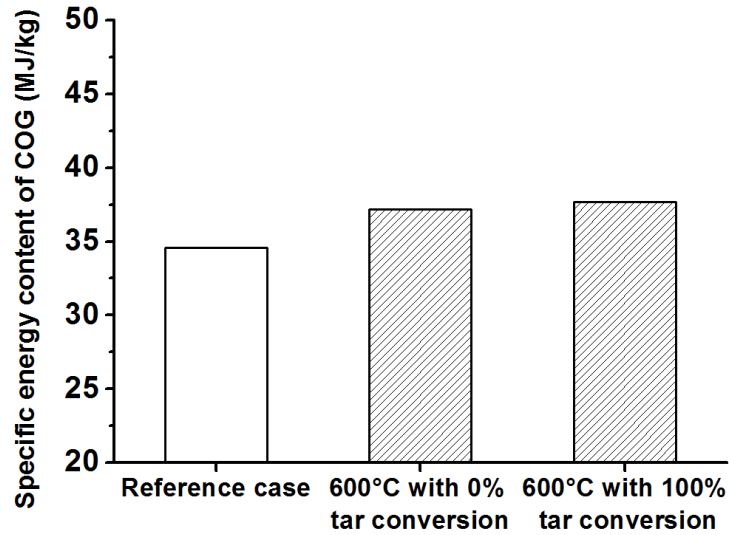
COG composition (vol%)	150% slag	100% slag	50% slag
H ₂ O	9.7	10.0	10.3
H ₂	64.7	64.4	64.0
CH ₄	18.3	18.1	17.9
CO	3.4	3.5	3.7
CO ₂	1.4	1.5	1.6
N ₂	2.2	2.2	2.2
C ₂ H ₄	0.00	0.00	0.00
C ₂ H ₆	0.00	0.00	0.00
C ₃ H ₆	0.00	0.00	0.00
H ₂ S	0.25	0.25	0.26
NH ₃	0.01	0.01	0.01
Tar	0.0	0.0	0.0
Deposited carbon (kg per tonne of steel)	21.7	21.6	21.6

262 Table 4 shows the gas composition of the reformed COG and the amount of deposited carbon on the
 263 slag for different amounts of slag participating in the reaction and assuming 100% tar conversion. The
 264 simulation results, however, are based on pure thermodynamics, rather than kinetics, of the tar
 265 reforming reaction and thus should be interpreted accordingly. Indeed, the results indicate no

266 significant change to the COG composition or carbon deposition for varied amounts of slag. This
267 suggests that from a purely thermodynamic point of view, the amount of slag has little effect on the
268 COG quality and extent of carbon deposition. This is partly explained by the low free CaO content in
269 the slag which leads to low absorption rates of CO₂/CO in the COG and thus a limited variation in the
270 COG composition. Nevertheless, due to the catalytic effect of the slag on tar reforming, literature has
271 shown that the extent of carbon deposition was significantly affected by the amount of slag present in
272 the reaction [19]. The quantification of such effect was investigated by experimental studies, the results
273 of which are presented in section 3.2.

274 Figure 7 shows the improved energy content of the COG in the SCAP process compared with that of
275 the reference case (i.e. the COG before entering the tar reformer). It was found that the energy content
276 of COG increased by up to ~9% using the SCAP process, of which only 1.5% of the increase is
277 attributed by tar decomposition. The low increment of COG energy content contributed by tar
278 decomposition can be explained by the relatively low fraction of tar (~13 wt%) in the raw COG. It
279 implies that the expectation of solely relying on tar decomposition to improve COG quality is
280 impractical. Instead, COG reforming assisted with tar decomposition and carbon deposition is the main
281 route for obtaining a hydrogen-enriched COG. The above discussion is also supported by the literature
282 [21] which reports that only 2.3% of the total exergy input of the steel making process is retained in the
283 tar, while a significant fraction (about 24%) of the total exergy is found in the combustible off-gases
284 (mainly COG and BFG). Thus, this leads future research efforts to examining the effect of COG

285 reforming temperature on carbon deposition and gas quality (to be studied in our future journal
286 publications).



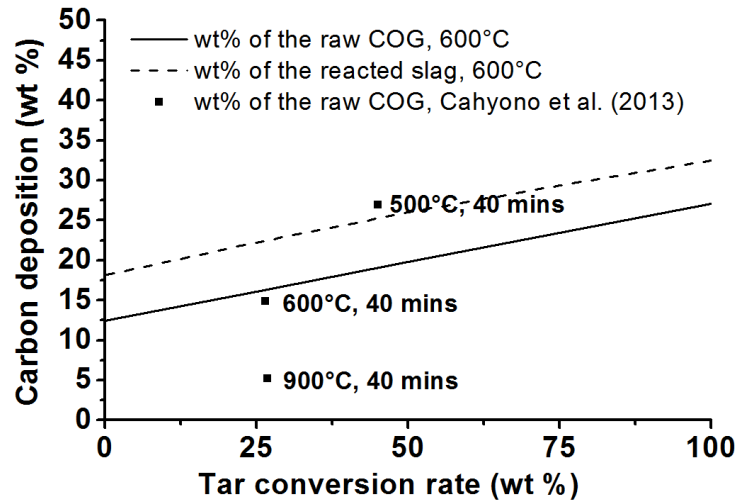
287

288 Figure 7: Specific energy content of COG before (i.e. the reference case) and after the tar reformer at a
289 reforming temperature of 600°C.

290 3.1.3 Carbon deposition

291 Figure 8 gives the extent of carbon deposition in terms of weight fraction of the reacted slag/raw COG
292 as a function of tar conversion rate at a reforming temperature of 600°C. It can be seen that with nil tar
293 conversion the carbon derived solely from the COG can reach approximately 12.5 wt% of the raw COG
294 or 18.1 wt% of the reacted slag. Increasing the tar conversion rate from 0 % to 100 % was found to
295 yield nearly 100 % more carbon. This indicates that tar decomposition is another significant source of
296 carbon despite its minimal contribution to the improved COG quality. In addition, to validate our
297 simulation results against the experimental data presented in the literature, we found that at a reforming
298 temperature of 600°C and a tar conversion rate of ~26% the simulation predicted a similar amount of
299 deposited carbon (~16 wt% of the raw COG) with experimental data [19] (see the black dot in Figure 8

300 at 600°C and 40 mins). For the readers' information, other literature experimental data obtained at
 301 500°C and 900°C for a reaction period of 40 mins are also presented in Figure 8.



302
 303 Figure 8: Carbon deposition as a function of tar conversion rate at a reforming temperature of 600°C,
 304 compared with some experimental data in the literature.

305 Table 5 shows the coke saving potential per tonne of steel production due to the recycling of the
 306 deposited carbon in the SCAP process at a tar reforming temperature of 600°C. It shows that compared
 307 to the conventional steelmaking process, the SCAP process can directly help reduce coke usage by 4.6 -
 308 9.9 wt% depending on the tar conversion extent. Upon full utilisation of the excess heat generated in
 309 the SCAP process, a further indirect coke saving of 2.7 – 2.9 wt% can be achieved. The total maximum
 310 amount of coke saving per tonne of steel production was thus estimated to be 12.8 wt%, namely 31.7
 311 kg coke per tonne of steel.

312 Table 5: Direct and indirect coke saving potentials per tonne of steel produced in SCAP process
 313 compared to the conventional steelmaking process (tar reforming temperature: 600°C).

Tar conversion rate (%)	Conventional coke usage (kg)	Carbon deposition (kg)	Direct coke saving per tonne of steel* (wt%)	Indirect^ coke saving per tonne of steel (wt%)	Total maximum coke saving per tonne of steel (wt%)
-------------------------	------------------------------	------------------------	--	--	--

100	248	21.6	9.9	2.9	12.8
75	248	18.7	8.6	2.8	11.4
50	248	15.8	7.3	2.8	10.0
25	248	12.9	5.9	2.7	8.6
0	248	10.0	4.6	2.7	7.2

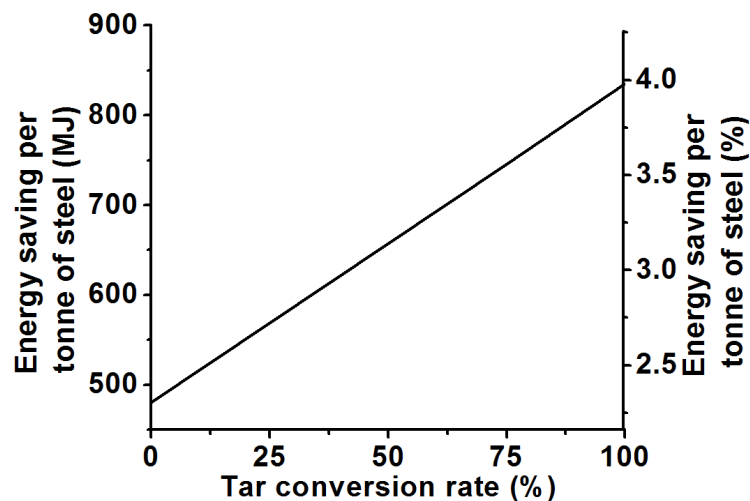
314 *. Assuming the energy contents of coke and carbon are 29 MJ/kg and 33 MJ/kg, respectively.

315 ^ Indirect coke saving is related to the equivalent amount of coke that may be saved if the total thermal energy excess
316 generated in the SCAP process is fully recycled back to the process. The thermal energy excess includes heat production in
317 the tar reformer and heat embedded in the hot slag product and the reformed COG, which are generally not available for
318 recovery in the conventional steelmaking process.

319

320 3.1.4 Energy saving and emission reduction

321 To better understand the advantages of the SCAP process, here we calculated the theoretical maximum
322 energy saving and emission reduction of the SCAP process compared to those of the conventional
323 steelmaking process (i.e. ~21 GJ and 1.8 tonne CO₂ emissions per tonne of steel) (see Figure 9). Figure
324 9 shows that at a tar reforming temperature of 600°C, the maximum energy saving of the SCAP process
325 was between 480 MJ and 850 MJ per tonne of steel depending on tar conversion extent. This equates to
326 approximately 2.3 – 4 % of the total energy intensity of conventional steelmaking process. The
327 associated maximum carbon emissions reduction was calculated to be about 3.2 % to 5.7 %.



328

329 Figure 9: Energy saving potential of SCAP process per tonne of steel production for a tar reforming
330 temperature of 600°C.

331 **3.2 TGA-FTIR evaluation of coal and slag mixtures**

332 The differential thermo-gravimetric (DTG) curves for each of the different coal to slag ratios are
333 presented in Figure 10. It can be seen that pyrolysis of coal alone resulted in a single peak in the DTG
334 curve at approximately 450°C attributed to primary devolatilisation of coal due to thermal
335 decomposition of its structure. For the coal and slag mixtures, this same peak was also apparent at
336 approximately 450-455°C but with decreasing intensity as the amount of slag increased. This may be
337 caused by an increasing amount of **chemical adsorption of CO₂ via carbonation reactions on the surface**
338 **of the slag components** as the amount of slag increases, which leads to less volatile weight losses as
339 coal decomposes. The amounts of CO₂ **adsorbed** by free CaO and FeO components of the slag start to
340 release this CO₂ at approximately 500°C and 650°C and peak at approximately 570°C and 800°C,
341 respectively. The peak at ~340-350°C may be attributed by the liberation of inter-molecular water
342 formed during hydration of CaO in the presence of wet coal at lower temperatures [32].

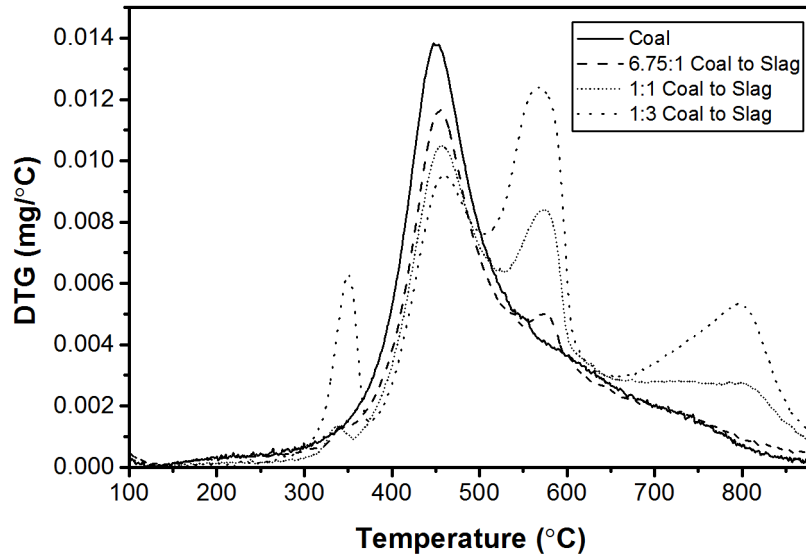


Figure 10: DTG curves for coal and three different coal to slag ratios.

343

344

345

346

347

348

349

350

351

352

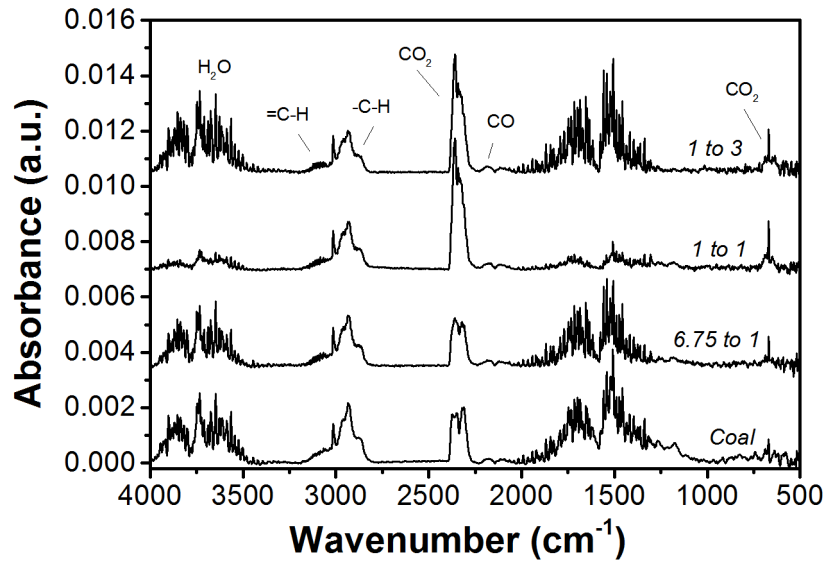
353

354

355

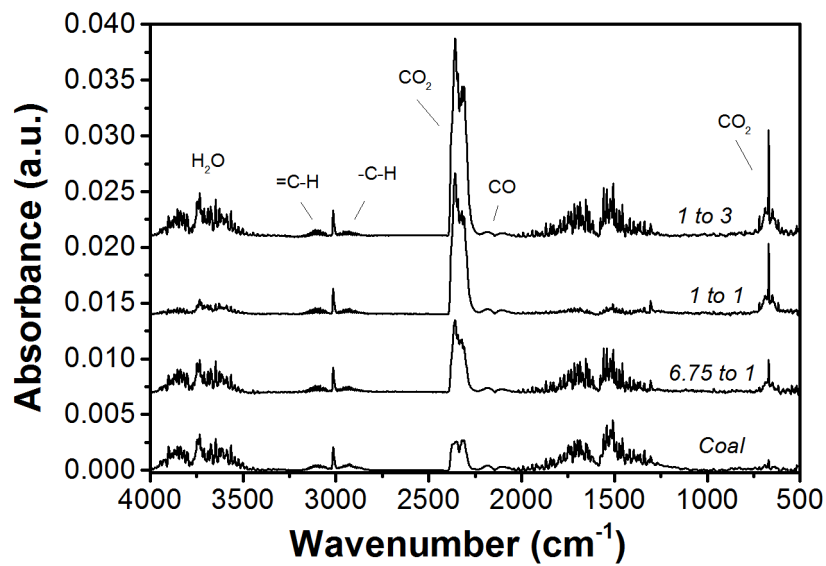
356

For each of the significant peaks in the DTG curves presented in Figure 10 at temperatures of 450, 570 and 800°C, the corresponding FTIR spectra for each of the different coal/slag treatments are presented in Figure 11, Figure 12 and Figure 13 respectively. At 450°C (Figure 11), the primary volatile constituents observed were CO₂ (~2400 cm⁻¹), CO (~2100 cm⁻¹), H₂O (~3700 cm⁻¹) as well as aliphatic and aromatic C-H (~2900-3200 cm⁻¹). At 570°C (Figure 12), the primary volatile constituents observed were CO₂ (~2400 cm⁻¹), CO (~2100 cm⁻¹), and to a lesser extent aliphatic and aromatic C-H (~2900-3200 cm⁻¹). At 800°C (Figure 13), the primary volatile constituents observed were CO₂ (~2400 cm⁻¹), and CO (~2100 cm⁻¹), with the aliphatic and aromatic C-H (~2900-3200 cm⁻¹) compounds no longer observed in the gaseous phase. These findings are expected as more tar components will decompose as temperature increases. For a more complete view of FTIR spectra variation as a function of temperature, the overall volatile evolution profile via FTIR is presented in Figure 14 for the coal to slag ratio of 1 to 1.



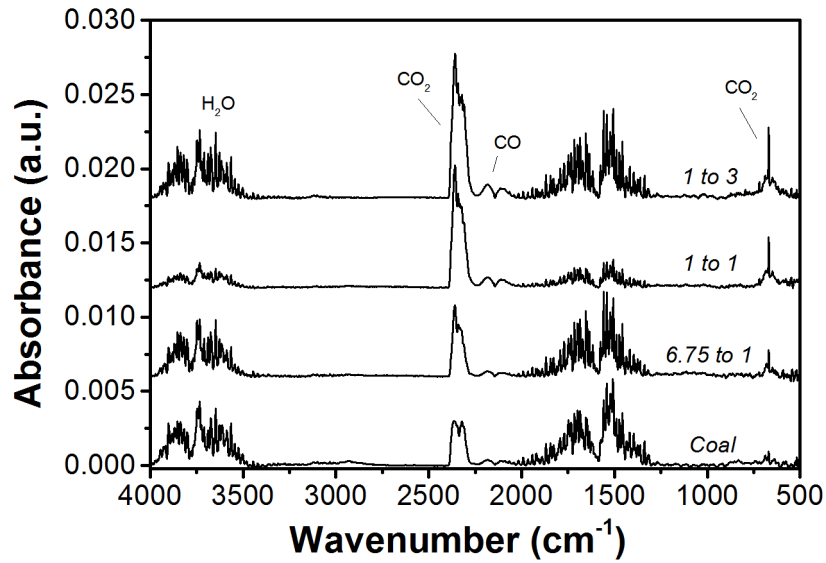
357

358 Figure 11: Online-FTIR gas analysis of three different coal to slag ratios at 450°C; Coal pyrolysis alone,
 359 6.75:1 coal to slag, 1:1 coal to slag and 1:3 coal to slag.



360

361 Figure 12: Online-FTIR gas analysis of three different coal to slag ratios at 570°C. Coal pyrolysis alone,
 362 6.75:1 coal to slag, 1:1 coal to slag and 1:3 coal to slag.



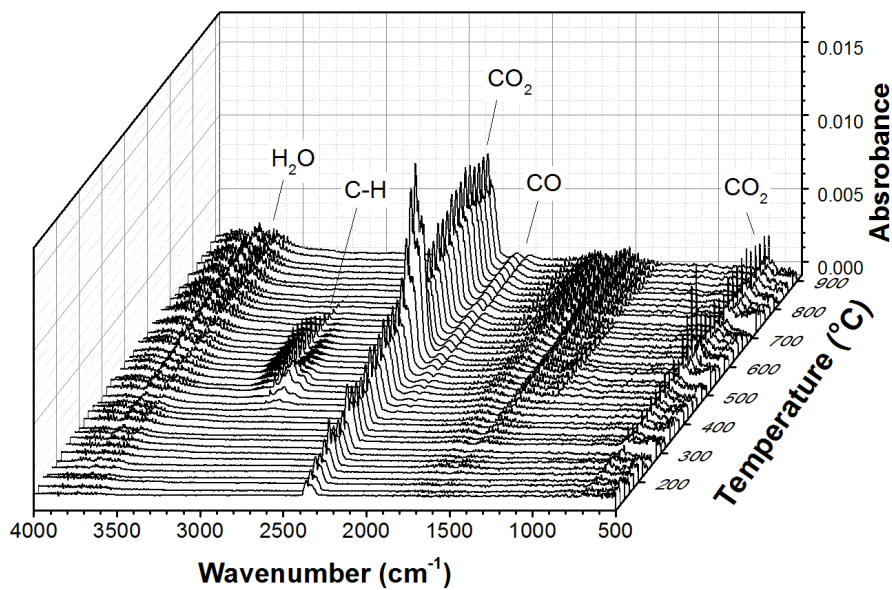
363

364 **Figure 13: Online-FTIR gas analysis of three different coal to slag ratios at 800°C. Coal pyrolysis alone,**
 365 **6.75:1 coal to slag, 1:1 coal to slag and 1:3 coal to slag.**

366 Over the entire temperature range it can be seen that the primary volatile constituents observed were

367 CO₂ (~2400 cm⁻¹), CO (~2100 cm⁻¹), and aliphatic/aromatic C-H (~2900-3200 cm⁻¹) compounds. This

368 figure



369

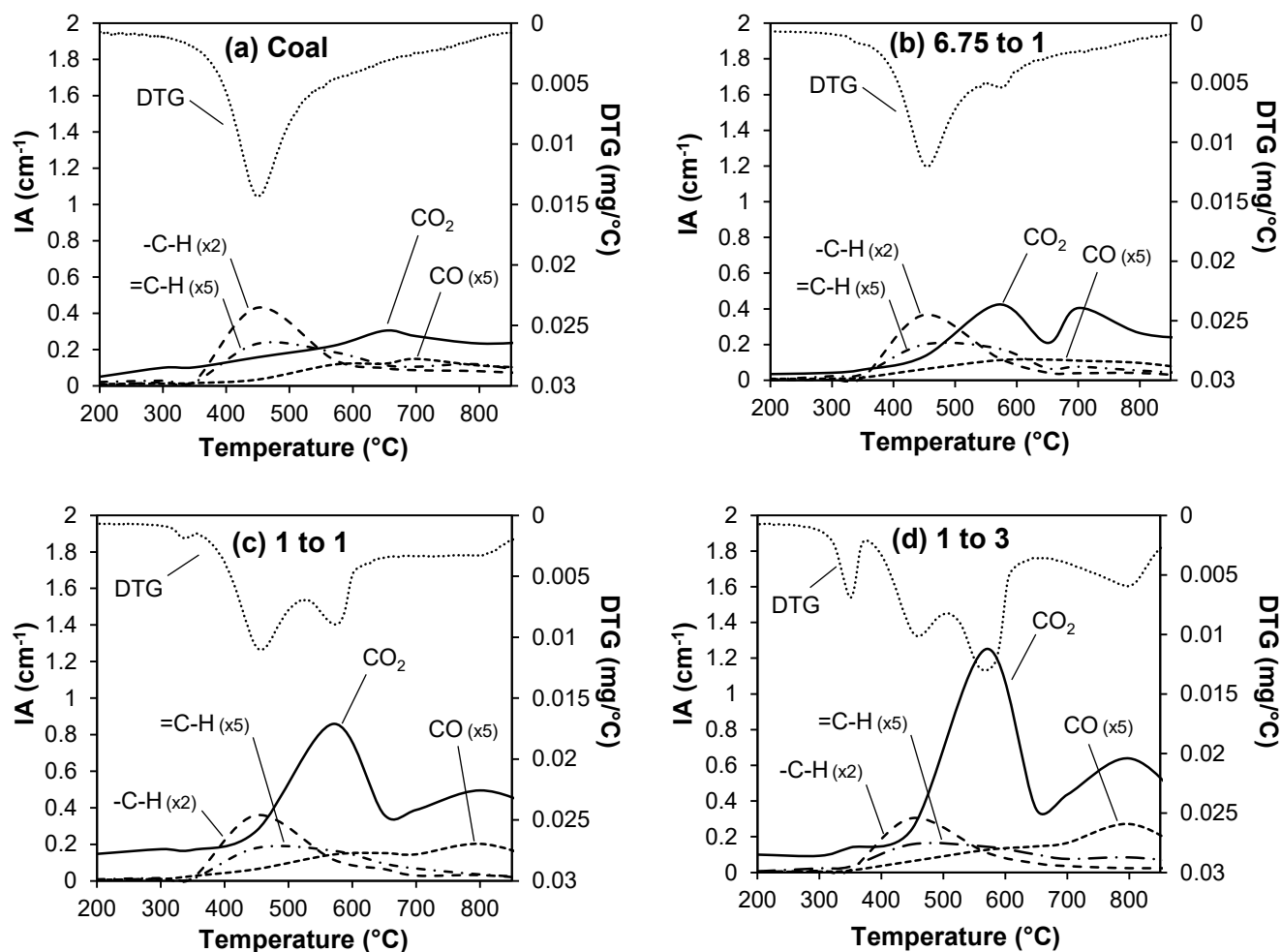
370 **Figure 14: FTIR volatile evolution profile for a coal to slag ratio of 1:1.**

371 On the other hand, Figures 11-13 also show that as more slag is introducing into the system the peaks
372 of major tar components (aliphatic and aromatic C-H) slightly decrease while that of CO₂ greatly
373 increases. This indicates that a greater amount of tar was decomposed into lighter components (e.g.
374 CO₂) as more slag was presented. To investigate this effect in a more quantitative manner, we used
375 similar methods to those presented in literature [33-35] and calculated the integrated absorbance under
376 the curve for different components in the gaseous phase (i.e. quantifying the changes in species
377 concentration). The definitions of the wavelength intervals for each of the species are detailed in Table
378 6.

379 Table 6: Wavenumber interval definitions for integrated area plots.

Species	Wavenumber range (cm ⁻¹)
CO	2140 - 2240
CO ₂	2241 - 2400
-C-H (aliphatics)	2800 - 3024
=C-H (aromatics)	3025 - 3200

380 Using the wavenumber assignments (Table 6), the area under the curve for each of the intervals was
381 calculated for each species as presented in Figure 15. In Figure 15, the curves for =C-H and CO have
382 been multiplied by a factor of five, while the -C-H curve has been multiplied by a factor of two in
383 order to discern the trends in the curve with increasing temperature.



384 Figure 15: Qualitative gaseous product evolution via integrated absorbance and derivative weight for
 385 four different coal to slag ratios; (a) coal pyrolysis, (b) coal to slag ratio of 6.75:1, (c) coal to slag ratio
 386 of 1:1 and (d) coal to slag ratio of 1:3.

387 For coal pyrolysis alone (Figure 15a), the release of aromatic ($=C-H$) and aliphatic ($-C-H$)
 388 hydrocarbons and CO_2 were primarily observed at the single peak in the DTG curve at $450^\circ C$. As the
 389 temperature increased the release of $-C-H$ and $=C-H$ groups decreased, while CO_2 and CO release
 390 increased, reaching maximums at $650^\circ C$ and $700^\circ C$ respectively.

391 In Figure 15a, b & c it can be seen that the addition of slag to the pyrolysis process had a direct effect on
 392 the gas evolution profile. The evolution of aromatic ($=C-H$) and aliphatic ($-C-H$) hydrocarbons
 393 occurred at approximately the same temperature, $450^\circ C$, for all coal to slag ratios, however the peak

394 intensity slightly decreased with increased slag content, signifying the catalytic effects of the slag. The
395 total amount of CO₂ and CO released dramatically increased with the introduction of slag. The peak in
396 CO evolution at approximately 800°C for coal to slag ratios of 1:1 (Figure 15c) and 1:3 (Figure 15d)
397 were attributed to the higher concentrations of CO₂ reacting with carbon contained in char or deposited
398 on the surface of slag via the following reaction:



400 The increase in CO₂ observed is indicative of slag reacting with hydrocarbon and oxygenated
401 compounds released during primary devolatilisation to form CO₂. At temperatures below 500°C, this is
402 then trapped by the CO₂ scavengers in the slag i.e. calcium and iron. As the temperature increased, the
403 CO₂ initially captured was released due to changes in the CO₂ equilibrium partial pressure. The release
404 of CO₂ occurred primarily at 570°C and above 700°C, which is characteristic of the calcination of the
405 calcium and iron rich components of the slag respectively. The absence of similar quantities of CO₂ and
406 CO for the pyrolysis of coal alone (Figure 15a) compared to other figures clearly indicates that the
407 presence of slag has the ability to catalyse tar cracking reactions to form the lower molecular weight
408 species identified such as CO₂ and CO. The greatest extent of catalysis was observed for the highest
409 slag to coal ratio of 3:1 where the greatest amount of CO₂ and CO were released.

410

411 **4 CONCLUSION**

412 A novel slag carbon arrestor process using steelmaking slag was proposed for energy recovery in the
413 steelmaking industry. In the SCAP process energy recovery can be achieved by utilising the energy
414 embedded in the hot raw COG while the tar reforming process is able to produce a carbon-rich slag and
415 a higher quality COG product. The results indicate that with SCAP process the COG energy content
416 can be increased from ~34.6 MJ/kg to ~37.7 MJ/kg (or by 9%). Also, recycling the carbon-rich slag in
417 the sinter machine and blast furnace can help reduce coke usage in the conventional steelmaking
418 process by up to ~12.8 wt%. This translates into a theoretical maximum energy saving of 4 % and a
419 carbon emission reduction of 5.7 % of the conventional steelmaking process. Moreover, our
420 preliminary experimental investigations have provided first-hand evidence of the catalytic ability of
421 slag for use in the SCAP process.

422

423 **ACKNOWLEDGEMENT**

424 The authors wish to acknowledge the financial support they have received from Australian Research
425 Council (ARC) and the University of Newcastle, Australia.

426

427 **References**

428 [1] M. Larsson, J. Dahl. Reduction of the specific energy use in an integrated steel plant-the effect of an
429 optimisation model. ISIJ international. 43 (2003) 1664-73.

- 430 [2] Bluescope Steel. Energy use in bluescope steel's steelmaking.
- 431 [3] Bluescope Steel. Reusing the by-products of the steel industry.
- 432 [4] B. Moghtaderi. Hydrogen enrichment of fuels using a novel miniaturised chemical looping steam
433 reformer. *Chemical Engineering Research and Design*. 90 (2012) 19-25.
- 434 [5] B. Moghtaderi, E. Doroodchi. Performance characteristics of a miniaturised chemical looping steam
435 reformer for hydrogen enrichment of fuels. *International Journal of Hydrogen Energy*. 37 (2012)
436 15164-9.
- 437 [6] K. Shah, C. Zhou, H. Song, E. Doroodchi, B. Moghtaderi. A novel chemical looping oxy combustor
438 process for combustion of solid and gaseous fuels: Thermodynamic analysis. *Energy & Fuels*. In press
439 (2014).
- 440 [7] C. Zhou, E. Doroodchi, B. Moghtaderi. An in-depth assessment of hybrid solar–geothermal power
441 generation. *Energy Conversion and Management*. 74 (2013) 88-101.
- 442 [8] C. Zhou, E. Doroodchi, B. Moghtaderi. Assessment of geothermal assisted coal-fired power
443 generation using an Australian case study. *Energy Conversion and Management*. 82 (2014) 283-300.
- 444 [9] C. Zhou, K. Shah, E. Doroodchi, B. Moghtaderi. Equilibrium thermodynamic analyses of methanol
445 production via a novel Chemical Looping Carbon Arrestor process. *Energy Conversion and*
446 *Management*. 96 (2015) 392-402.
- 447 [10] C. Zhou, K. Shah, B. Moghtaderi. Techno-Economic Assessment of Integrated Chemical Looping
448 Air Separation for Oxy-Fuel Combustion: An Australian Case Study. *Energy & Fuels*. 29 (2015) 2074-
449 88.
- 450 [11] M. Onozaki, K. Watanabe, T. Hashimoto, H. Saegusa, Y. Katayama. Hydrogen production by the
451 partial oxidation and steam reforming of tar from hot coke oven gas. *Fuel*. 85 (2006) 143-9.

- 452 [12] P. Diemer, H.-J. Killich, K. Knop, H.B. Lungen, M. Reinke, P. Schmöle. Potentials for utilization
453 of coke oven gas in integrated iron and steel works. *Stahl und eisen*. 124 (2004) 21.
- 454 [13] L. Haoguan. Further Processing of Coal Tar Based Pitch [J]. *Chemical Technology Market*. 8
455 (2000) 002.
- 456 [14] B. Yue, X. Wang, X. Ai, J. Yang, L. Li, X. Lu, et al. Catalytic reforming of model tar compounds
457 from hot coke oven gas with low steam/carbon ratio over Ni/MgO–Al₂O₃ catalysts. *Fuel Processing*
458 *Technology*. 91 (2010) 1098-104.
- 459 [15] C. Shi. Steel slag-its production, processing, characteristics, and cementitious properties. *Journal*
460 *of Materials in Civil Engineering*. 16 (2004) 230-6.
- 461 [16] T. Ariyama, M. Sato. Optimization of ironmaking process for reducing CO₂ emissions in the
462 integrated steel works. *ISIJ international*. 46 (2006) 1736-44.
- 463 [17] G. Bisio. Energy recovery from molten slag and exploitation of the recovered energy. *Energy*. 22
464 (1997) 501-9.
- 465 [18] E. Worrell, L. Price, N. Martin. Energy efficiency and carbon dioxide emissions reduction
466 opportunities in the US iron and steel sector. *Energy*. 26 (2001) 513-36.
- 467 [19] R. Bakti Cahyono, A.N. Rozhan, N. Yasuda, T. Nomura, S. Hosokai, Y. Kashiwaya, et al.
468 Integrated coal-pyrolysis tar reforming using steelmaking slag for carbon composite and hydrogen
469 production. *Fuel*. 109 (2013) 439-44.
- 470 [20] K.V. Shah, M.K. Cieplik, C.I. Betrand, W.L. van de Kamp, H.B. Vuthaluru. Correlating the
471 effects of ash elements and their association in the fuel matrix with the ash release during pulverized
472 fuel combustion. *Fuel Processing Technology*. 91 (2010) 531-45.
- 473 [21] A. von Gleich, R.U. Ayres, S. Goessling-Reisemann. Sustainable metals management; securing
474 our future, steps towards a closed loop economy. Springer2006.

- 475 [22] V.I. Shatokha, O.O. Gogenko, S.M. Kripak. Utilising of the oiled rolling mills scale in iron ore
476 sintering process. *Resources, Conservation and Recycling*. 55 (2011) 435-40.
- 477 [23] M. Platts. The coke oven by-product plant.
- 478 [24] U. Yadav, B. Das, A. Kumar, H. Sandhu. Solid Wastes Recycling through Sinter-Status at Tata
479 Steel, Jamshedpur-831001. 2002.
- 480 [25] U.S. Department of Energy. Steel technology roadmap, second edition - Chapter 3 iron unit
481 recycling. 2001.
- 482 [26] P. Diemer, H.-J. Killich, K. Knop, H.B. Lungen, M. Reinke, P. Schmöle. Potentials for utilization
483 of coke oven gas in integrated iron and steel works. 2nd International Meeting On Ironmaking, Vitoria,
484 Espirito Santo, Brazil, 2004.
- 485 [27] K. Wright. The coke oven managers' year book - coke oven gas treatment tar, liquor, ammonia.
- 486 [28] R.B. Cahyono, N. Yasuda, T. Nomura, T. Akiyama. Optimum temperatures for carbon deposition
487 during integrated coal pyrolysis–tar decomposition over low-grade iron ore for ironmaking
488 applications. *Fuel Processing Technology*. 119 (2014) 272-7.
- 489 [29] P.J. Kirton, J. Ellis, P.T. Crisp. The analysis of organic matter in coke oven emissions. *Fuel*. 70
490 (1991) 1383-9.
- 491 [30] C.N. Hamelinck, A.P.C. Faaij, H. den Uil, H. Boerrigter. Production of FT transportation fuels
492 from biomass; technical options, process analysis and optimisation, and development potential. *Energy*.
493 29 (2004) 1743-71.
- 494 [31] Directorate-General for Research and Innovation European Commission. Summary report on RTD
495 in iron and steel slags development and perspectives. in: R. Tomellini, (Ed.). *Technical steel research*
496 *workshop*, Bilbao, Spain, 1999.

- 497 [32] Ngamcharussrivichai, C.; Wiwatnimit, W.; Wangnoi, S., Modified dolomites as catalysts for palm
498 kernel oil transesterification. *J. Mol. Catal. A: Chem.* 2007, 276, (1–2), 24-33.
- 499 [33] –Biagini, E.; Barontini, F.; Tognotti, L., Devolatilization of Biomass Fuels and Biomass
500 Components Studied by TG/FTIR Technique. *Ind. Eng. Chem. Res.* 2006, 45, (13), 4486-4493.
- 501 [34] Zhang, H.; Zheng, J.; Xiao, R.; Jia, Y.; Shen, D.; Jin, B.; Xiao, G., Study on Pyrolysis of Pine
502 Sawdust with Solid Base and Acid Mixed Catalysts by Thermogravimetry–Fourier Transform Infrared
503 Spectroscopy and Pyrolysis–Gas Chromatography/Mass Spectrometry. *Energy Fuels* 2014, 28, (7),
504 4294-4299.
- 505 [35] Yan, J.; Jiang, X.; Han, X.; Liu, J., A TG–FTIR investigation to the catalytic effect of mineral
506 matrix in oil shale on the pyrolysis and combustion of kerogen. *Fuel* 2013, 104, 307-317.